

Deep optical observations of the fields of two nearby millisecond pulsars with the VLT *

F. K. Sutaria¹, A. Ray², A. Reisenegger³, G. Hertling³, H. Quintana³, and D. Minniti³

¹ Dept. of Physics and Astronomy, The Open University, Milton Keynes, U.K.

² Tata Institute of Fundamental Research, Mumbai, India.

³ Dept. of Astronomy and Astrophysics, Pontificia Universidad Católica de Chile, Santiago, Chile.

Received ; Accepted

Abstract. An abstract should be given

1. Introduction

Optical pulses from the Crab pulsar were detected by Cocke, Disney and Taylor (1969) within a year of the discovery of the pulsar in the radio band (Staelin & Reifenstein, 1968) and the inauguration of the field of pulsars by S. Jocelyn Bell and collaborators (Hewish et al. 1968). Since then, the number of pulsars discovered in the radio band has gone up to nearly 1400 (ATNF pulsar catalogue), but the number of pulsed counterparts detected in the high-energy bands remains small. To date, in the optical bands, these remain 5, (Shearer & Golden 2002), and in the X-ray band 22, including 6 millisecond pulsars (MSP) (Becker & Aschenbach 2002). Multi-wavelength detection of rotation-powered neutron stars provides observational input to the nature of the underlying mechanism of pulsar radiation, whether it is of thermal origin or due to radiation from accelerated particles in its magnetosphere (see e.g. Pavlov, Stringfellow, & Cordova 1996).

Millisecond pulsars (MSP) are a special class, not only because of their short spin periods, but also because of their smaller surface magnetic field, old age, and evolutionary history of spin-up due to accretion of mass and angular momentum from a binary companion (Alpar et al., 1982). In the process, the star may have been resurrected from a state of hibernation into one of detectable pulsed radio emission. They represent a considerable extension of the parameter space of classical pulsars, so different radiation mechanisms may well be active in their magnetospheres. Their old age means that they have almost certainly radiated away any “fossil” heat from their original collapse or from their accretion epoch.

Thus, any thermal emission must be due to external re-heating from the magnetosphere or to internal dissipation mechanisms, most likely related to the star’s slowing rotation rate (see, e.g., Cheng et al. 1992, Reisenegger 1995, Larson & Link 1999, and references therein).

While MSP with binary companions are interesting in their own right from the evolutionary angle, radiation from the companions, even if they are low-mass old white dwarfs, “contaminates” the faint high-energy radiation intrinsic to the pulsar itself. This is especially true of the optical and ultraviolet regions. It is therefore of interest to concentrate on the isolated pulsars to study their radiative properties in these bands. Isolated MSPs are relatively rare objects — till mid-2002, only 10 have been detected in the Galactic plane. By contrast, the number of galactic MSPs (outside globular clusters) totals ~ 57 . None of the optically detected pulsars is an isolated MSP, which might at least partly be due to a lack of sufficiently deep exposures. The advent of the VLT class of telescopes is therefore a crucial technological development for these faint objects.

The pulsed high-energy radiation from a rotation powered (isolated) pulsar is a combination of differing amounts of three spectral components: 1) power law emission resulting from particles accelerated in the magnetosphere, 2) a soft black-body component from the surface of a cooling neutron star, and 3) a hard thermal component associated with heated polar caps bombarded by energetic particles. Measurements of the radiative fluxes and spectra in different bands can constrain the relative weights of these components.

In this paper, we present the results of deep VLT observations of two southern, isolated millisecond pulsars, PSR J1024-0719 and PSR J1744-1134, which are among the closest MSPs discovered and which have also been detected in the X-ray band by ROSAT. Identification

* Based on observations with the ESO 8.2m VLT-Antu (UT1) Telescope under Program 66.D-0448 and 67.D-0538

Correspondence to: areisene@astro.puc.cl

of candidate objects in the optical band forms the first step towards searches for optical pulsations from a pulsar. These pulsars have some of the highest spin-down flux ($\dot{E}_{rot}/4\pi d^2 = I\Omega\dot{\Omega}/4\pi d^2$) among millisecond pulsars, an indicator of their propensity to produce high-energy radiation. Because of their proximity as well as low extinction in their direction, they are among the best candidates for optical detection. In Sect. 2, we discuss what is known about these two pulsars in the X-ray and radio bands. We next present, in Sect. 3, the VLT service mode observations and their data analysis. In Sect. 4, we discuss the results obtained from the VLT data. We supplement our discussion of a star near PSR J1024-0719 with a spectroscopic observation with the Magellan I Baade 6.5 m telescope at Las Campanas Observatory. In Sect. 5, we discuss the multi-band optical results in the context of high-energy and radio emission from the pulsars and compare these with those from slower pulsars, and theoretical models of pulsar radiation. We give our conclusions in Sect. 6.

2. Radio and X-ray properties of the two pulsars

Both PSR J1744-1134 and PSR J1024-0719 were first detected in the radio bands as isolated MSP with periods $P = 4.07$ and 5.16 ms, respectively (Bailes et al. 1997). In Tab. 1 we quote some characteristics of these objects relevant to our observations and their interpretation. The astrometric data and the proper motions were determined by radio timing observations (Toscano et al. 1999a).

The radio pulse profile of PSR J1744-1134 is narrow and sharply peaked, with a duty cycle of $\sim 10\%$, while PSR J1024-0719 exhibits a broad, multiply peaked profile with a duty cycle of $\sim 50\%$. The radio and X-ray emission are most likely based on different physical mechanisms: curvature radiation from e^\pm pairs near the NS surface (Ruderman & Sutherland 1975), and synchrotron radiation from energetic particles in the outer gap (Cheng, Ho, & Ruderman 1986), respectively. However, at least in the case of PSR B1821-24 (another MSP), RXTE observations (Rots et al. 1997) show that the leading edge of the most energetic pulse coincides with the radio pulse profile at 800 MHz, possibly implying a common site for the origin of the two pulses.

Nevertheless, the two pulsars are similar in that the spin-down ages for both objects are $\tau \equiv P/(2\dot{P}) > 10^9$ yr (Tab. 1). Both pulsars are in the age bracket where non-thermal magnetospheric emission can be expected to dominate over any thermal effects, unless strong re-heating occurs. Some uncertainty exists over the distance estimate to the two pulsars. An upper limit to the distance of PSR J1744-1134, based on the assumption that the period derivative is entirely due to the transverse motion of the pulsar (Shklovskii effect), is 1910 pc (Toscano et al. 1999a). Based on parallax measurements of PSR J1744-1134, Toscano et al. 1999b estimate the distance d as 357^{+43}_{-35} pc. This number decreases to 166 pc (Bailes et al. 1997) if d is estimated using the measured value of the dispersion measure (DM) and values of elec-

tron densities from the Taylor & Cordes (1993) model. However, it is to be noted that, while this model adequately describes the properties of interstellar medium (ISM) at $d > 1$ kpc, it does not account properly for fluctuations in the local ISM. For our purposes, we use a distance estimate of 0.357 kpc for PSR J1744-1134. In the case of PSR J1024-0719, an upper limit of $d = 0.226$ kpc is obtained from the Shklovskii effect, while a $d = 0.35$ kpc is obtained by using DM and the Taylor and Cordes model (Toscano et al. 1999a). We shall adopt a value $d = 0.2$ kpc for PSR J1024-0719 in this paper, unless specified otherwise.

The corresponding X-ray counterparts for both pulsars were discovered by the ROSAT HRI (Becker & Trümper 1999; hereafter BT99). Because both pulsars are quite faint in this band, no timing observations could be done, and the counterparts were identified by their proximity to the radio positions. Assuming a photon spectral index $\alpha = 2$, these authors find that the unabsorbed X-ray luminosity of PSR J1744-1134 (scaled to our adopted distance) is $L_X = 4 \times 10^{29} (d/0.36\text{kpc})^2$, and that of PSR J1024-0719 is $L_X = 1 \times 10^{29} (d/0.2\text{kpc})^2$. The X-ray to spin-down luminosity ratios L_X/\dot{E}_{rot} are then 2×10^{-4} and 5×10^{-5} , respectively, somewhat below the general relation that Becker & Trümper 1997 found statistically among high-energy pulsars, $L_X/\dot{E}_{rot} \sim 10^{-3}$.

Table 1. Characteristics of PSRs J1024-0719 and J1744-1134 (BT99, Toscano et al. 1999a, Toscano et al. 1999b)

Property	PSR J1024-0719	PSR J1744-1134
Period (P) [ms]	5.16	4.07
\dot{P} [10^{-20}s^{-1}]	1.873(5)	0.89405(9)
\dot{E}_{rot} [erg s^{-1}]	5.25×10^{33}	1.90×10^{33}
d [kpc]	0.200	0.357
τ [10^9 yr]	27	9.1
B [10^8 G]	1.3	1.7
R.A. (J2000)	$10^h 24^m 38^s 7040(1)$	$17^h 44^m 29^s 390963(5)$
Dec. (J2000)	$-07^\circ 19' 18'' 849(3)$	$-11^\circ 34' 54'' 5746(5)$
P. M. (R.A.)	-41(2)	18.72(6)
[mas yr^{-1}]		
P. M. (Dec.)	-70(3)	-9.5(4)
[mas yr^{-1}]		
Epoch (MJD)	50456.0	50434.0
$L_X(0.2\text{-}2.4 \text{ keV})$ [erg s^{-1}]	$1 \times 10^{29} (d/200\text{pc})^2$	$4 \times 10^{29} (d/360\text{pc})^2$

3. The VLT observations

PSR J1744-1134 was observed by the ESO 8.2m Very Large Telescope Antu (VLT-UT1) with the FORS1 CCD in the narrow field imaging mode in the Bessel B, V and R bands on four nights during April 2001 (MJD 52017-52027). PSR J1024-0719 was observed by the same instruments/mode in the U, V, R and I bands within less than one hour in March 2001 (MJD 51996). Both sets of

observations were carried out in the service mode. A brief summary of the observations is provided in Tab. 2.

3.1. The observation

The photometric analysis for both objects was done using the MIDAS pipeline processed data. The pipeline processing ensures that each frame is checked for over-exposure and suitably bias-subtracted and flat-fielded, using the master bias and flats generated from calibrations observations made on each night. Finally, the prescan and overscan regions are removed from the science images used in this analysis.

Our initial examination of the DSS plates in the vicinity of PSR J1744-1134 showed no bright objects. However, the VLT images show a bright star with $V = 21.3$ about $2''$ from the position of the pulsar. Thus, in order to strike a balance between deep exposure and good seeing, of the twenty-three ten-minute exposures with Bessel B, we rejected the three exposures with the worst seeing taken on 2001 April 21, thus reducing the available photometry time to 3.33 hr. The available exposure time in each of the V and R filters was 48 min. The median seeing in the B, V and R filters was $0''.725$, $1''.095$ and $0''.795$ respectively.

For PSR J1024-0719, the available exposure time was 13.33 min in U, 6 min in both V and I, and 9 min in R (see table 2). The median seeing in the U, V, R and I frames was $0''.63$, $0''.97$, $0''.74$ and $0''.71$ respectively.

Table 2. Observation summary for VLT FORS1 CCD photometry

PSR	Filter	Exposure time	Mean air mass	Mean Seeing ["]
	(Bessel)	[s]		
J1744-1134	B	20×600	1.04	0.725
	V	2×540	1.06	1.095
		$+3 \times 600$		
	R	2×540	1.08	0.795
J1024-0719		$+3 \times 600$		
	U	1×900	1.2	0.63
	V	3×120	1.3	0.97
	R	3×180	1.2	0.74
	I	3×120	1.2	0.71

3.2. Data reduction

The image processing was done using the IRAF software. With the exception of the single image in the U-band, the reduced images in each filter were aligned and median-combined using a cosmic-ray rejection algorithm. Because in the case of both PSR J1024-0719 and PSR J1744-1134, there is a $V \sim 20 - 21$ star present within $\sim 1''.5 - 2''$ of the pulsar position, photometric analysis of the combined images was carried out using PSF-subtraction photometry (Massey & Davis 1992). In order to ensure that wings of the PSF of nearby stars are subtracted out cleanly, we

constructed a PSF for each frame, using only the brightest unsaturated stars, which were of magnitude a little brighter or close to that of the “contaminating star”. In general, we find that the PSF of the FORS1-CCD is position-dependent and is best fit by the IRAF moffat25 or penny1 functions with 2nd order variability in X and Y. Aperture correction was done on the CCD magnitudes, and the final magnitudes of all objects observed in the vicinity of the pulsar’s radio position were determined by comparison with standard stars. The standard stars used were from Landolt (1992) field SA109 for PSR J1024-0719, and fields SA109, SA110, and MARKA for PSR J1744-1134, observed on the same nights.

3.3. Astrometry

Correcting for the proper motion, the position of PSR J1744-1134 at the epoch of the the VLT observations was RA = $17^h 44^m 29\rlap{.}^s 39638(3)$, Dec = $-11^\circ 34' 54\rlap{.}'' 616(2)$, and that of PSR J1024-0719 was RA = $10^h 24^m 38\rlap{.}^s 6925(6)$, Dec = $-07^\circ 19' 19\rlap{.}'' 14(1)$.

Astrometric corrections to the observed CCD positions were carried out by comparison with both USNO-A2 catalog of astrometric standards (Monet et al. 1998) and the HST Guide Star II (GSCII) catalog. We report the results based on the more recent GSCII catalog, where the epoch of observation was from 1983-1986. The presence of nearby bright objects made it imperative to observe in the high-resolution mode. However, this reduced the number of GSCII astrometric standards in the field of view (FOV) of PSR J1024-0719 to only 6. The crowded field PSR J1744-1134 provided 14 astrometric standards within $1''.5$ of the pulsar position. The pixel coordinates of the reference stars were obtained from our photometric analysis, and they were converted to RA and Dec using the ASTROM package supplied with the STARLINK software.

For the field of PSR J1024-0719, the rms error in the fitting and transformations was $0''.12$ in RA and $0''.16$ in Dec. The average error in the positions of the relevant stars in the GSCII catalog is $0''.39$ in both directions. Thus, incorporating the error in the measurement of the proper motion, we estimate the total astrometric error in the observation of this field at $0''.42$ in RA and $0''.43$ in Dec. For PSR J1744-1134, the error in the astrometry of the GSCII stars is $0''.28$ in RA and $0''.30$ in Dec, and the error in the fitting and transformations is $0''.16$ and $0''.14$, respectively. In this case, the total astrometric error in the position is $0''.34$ and $0''.33$ in RA and Dec, respectively. We note that astrometry relative to the USNO-A2 catalog provides similar results, though the errors are slightly larger.

Since we use the radio pulsar positions to search for their optical counterparts, we need to consider the accuracy of the *radio timing* position with respect to the position in the optical frame. The GSCII catalog was calibrated using the Hipparcos and Tycho frames of reference, which are tied to the International Celestial Reference

Frame (ICRF, tied to the radio Very Long Baseline Interferometry, Ma et al. 1998).

An estimate of the absolute accuracy of pulsar radio timing positions was made by Fomalont et al. (1992) (and Fomalont et al. 1997) through comparing them with positions determined by interferometry. In general, they found the RA and Dec position offsets derived from timing and interferometric positions to be a function of the position of the target in the sky. Fomalont et al. (1992) state that, while there are no significant offsets between the coordinate frames in a global comparison of VLA positions and timing positions, there is a mean scatter of about $0''.8$ in each coordinate (RA and Dec).

If we add this to the above astrometric errors, then for both pulsars the total astrometric error in both RA and Dec would be $\approx 0''.9$, giving an error circle of radius $\approx 1''.3$. Therefore, any optical star-like emission within about $1''.5$ of the radio timing position should be taken with interest for further scrutiny, especially for time resolved photometry.

4. Results

The broadband magnitudes in multiple optical bands and astrometric positions of objects within $2''.0$ of the radio timing positions of our two target millisecond pulsars are reported in Tab. 3. We do not detect any object near PSR J1744-1134. An image of the field of view of this pulsar appears in Fig. 1.

Fig. 1. VLT FORS1 V-band field of view $40'' \times 40''$ centred about the radio timing position of PSR J1744-1134 (marked by the cross). North is to the top, and East to the left.

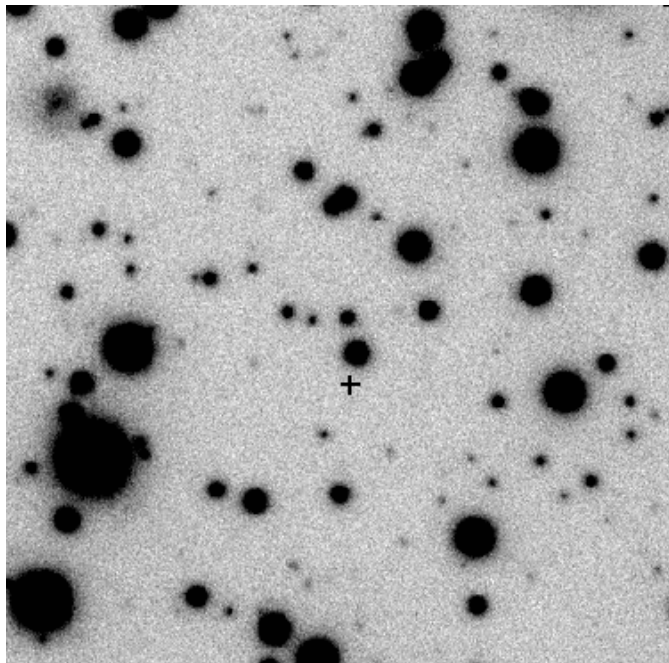
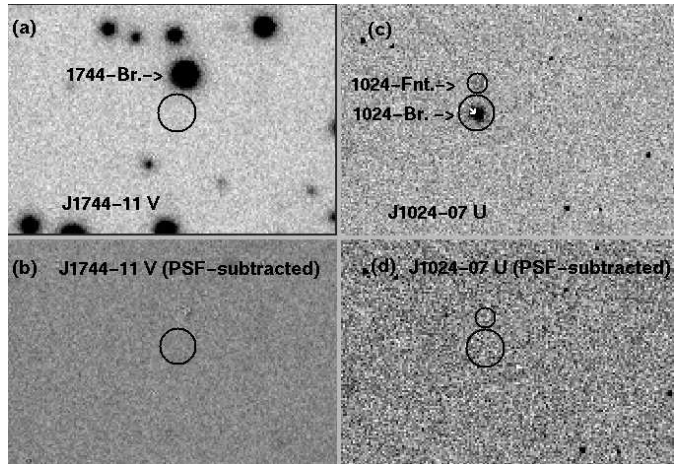


Fig. 2. Images (a) and (b) are the Field of View (FOV) of PSR J1744-1134 in V, before and after PSF-subtraction, respectively. The “error circle” of $1''$ is centered at the radio position of the PSR. Images (c) and (d) show the FOV of PSR J1024-0719 in U, before and after PSF-subtraction respectively. The position of the pulsar within the $1''$ “error circle” is marked by the small white arrow. The blue object 1024-Fnt is encircled within the smaller region, just north of 1024-Br.



Because of the presence of a $V = 21.34$ star close to the position of PSR J1744-1134, the limiting magnitude for the pulsar counterpart was estimated by introducing artificial stars at the pulsar position in each filter, by using the IRAF task `addstar`, and repeating PSF-subtraction photometry (see Fig. 2). Thus, the limiting magnitude for 3.5σ detection by the automatic star-finding algorithm `daophot` are $B = 26.9$, $V = 26.3$, and $R = 26.0$. We note that, from exposure-time considerations, the faintest object that could be detected in these frames would have $B = 28.0$, $V = 27.25$, $R = 26.8$ for a 4σ detection over the entire PSF.

For PSR J1024-0719, we find two objects within $1''.5$ of the radio position of the pulsar (see Fig. 2). The closer one, 1024-Br, only $\sim 0''.2$ away, has magnitudes $U = 22.11 \pm 0.03$, $V = 19.82 \pm 0.01$, $R = 18.89 \pm 0.01$, and $I = 18.17 \pm 0.01$. The other, substantially fainter object, 1024-Fnt, $\sim 1''.48$ north of the radio pulsar, has magnitudes $U = 23.8 \pm 0.1$, $V = 24.9 \pm 0.1$, $R = 24.4 \pm 0.1$ and $I = 24.2 \pm 0.2$. The reported magnitude errors for both objects include the intrinsic error in the Landolt catalogue and the error in photometry. The angular separation between the bright and faint objects is $1''.67$.

An object is reported close to the position of 1024-Br in various optical and infrared catalogs. The USNO-A2 catalog (Monet et al. 1998) gives magnitudes $B = 19.7$ and $R = 19.1$, DENIS (DENIS Consortium, 1998) reports $I = 18.0$, and 2MASS (IPAC/UMass, 2000) gives $J = 17.2$, $H = 16.1$, and $K = 16.5$). Applying astrometric corrections based on coincident stars within our field, we find the DENIS and 2MASS positions to agree with

our determination for 1024-Br to within $0.^{\circ}2$, whereas the USNO-A2 position is off by $+1.^{\circ}2$ in RA and $+2.^{\circ}0$ in Dec. The similarity in positions and magnitudes makes it almost unavoidable that the source is the same in all cases. The discrepancy in the USNO-A2 position (taken in 1953, whereas all other measurements are from 1995-2001) may be either an error or an indication of a proper motion of -25 mas yr^{-1} in RA and -40 mas yr^{-1} in Dec, almost identical in direction, but about 40% lower in magnitude, compared to the radio-timing-determined proper motion of PSR J1024-0719.

Table 3. Positions and magnitudes of optical point sources closest to the radio positions of two MSPs. The limiting magnitudes are also provided for 3.5σ detection at the central pixel in the exposure times used here for PSR J1744-1134

Object	Magnitude	PSR pos. - Obj. pos.	
		δ RA	δ Dec
J1744-1134 (upper lim.)	$B \geq 26.9, V \geq 26.3,$ $R \geq 26.0$	$0.^{\circ}0$	$0.^{\circ}0$
1744-Br	$B = 18.86, V = 21.34,$ $R = 19.91$	$+0.^{\circ}4$	$-2.^{\circ}0$
1024-Br	$U = 22.11, V = 19.82,$ $R = 18.89, I = 18.17$	$+0.^{\circ}1$	$-0.^{\circ}2$
1024-Fnt	$U = 23.8, V = 24.9,$ $R = 24.4, I = 24.2$	$-0.^{\circ}2$	$+1.^{\circ}5$

4.1. Extinction-corrected magnitudes and multi-waveband fluxes

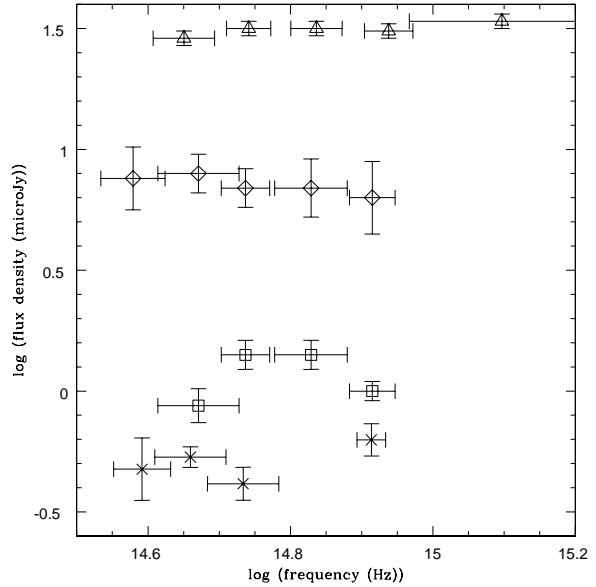
Based on the dispersion measures of the two pulsars, BT99 obtained hydrogen column densities in the directions of PSR J1024-0719 and PSR J1744-1134 as $N_H = 2 \times 10^{20} \text{ cm}^{-2}$ and $N_H = 1 \times 10^{20} \text{ cm}^{-2}$ respectively. In the ROSAT 0.1 – 2.4 keV band, their X-ray fluxes were both $f_X \sim 2 \times 10^{-14} \text{ erg s}^{-1} \text{ cm}^{-2}$. Using the scaling of de Boer et al. (1987) between visual extinction and hydrogen column density, $A_V = N_H / (1.79 \times 10^{21})$, we obtain $A_V = 0.11$ for PSR J1024-0719. The wavelength-dependent continuum absorption in the main photometric bands (Allen 2000) then gives, for the same pulsar, $A_U = 1.58A_V = 0.17$, $A_R = 0.749A_V = 0.08$, and $A_I = 0.479A_V = 0.05$.

The extinction-corrected magnitudes for 1024-Br, assuming it to be at the same distance as the pulsar, are $U = 21.94$, $V = 19.71$, $R = 18.81$, and $I = 18.12$. Similarly, the extinction-corrected magnitudes for 1024-Fnt are $U = 23.65$, $V = 24.83$, $R = 24.33$ and $I = 24.19$. For the latter, the corresponding flux densities (in μJy) at the frequencies corresponding to the centroids of the FORS1 broadband Bessel filters (FORS1 2000) are plotted in Fig. 3.

The corresponding extinction-corrected magnitude limits for PSR J1744-1134 are $B \geq 26.8$ (corresponding

Fig. 3. Optical photometry of pulsars. The top set (\triangle) is for the Crab pulsar with flux densities scaled down by a factor of 100 to fit in the graph. It also includes a measurement in the UV band at $\lambda\lambda 2400\text{A}$. Next is the LMC pulsar PSR 0540-69 (\diamond), followed by the Vela pulsar PSR 0833-45 (squares). Finally, at the bottom are extinction-corrected flux densities of the object 1024-Fnt (\times).

Optical emission (near): Crab, PSR0540-69, Vela, PSR1024-0719



to $0.079 \mu\text{Jy}$ at B-band centroid $7.0 \times 10^{14} \text{ Hz}$), $V \geq 26.2$, and $R \geq 26.0$.

4.2. Nature of the bright star close to PSR J1024-0719

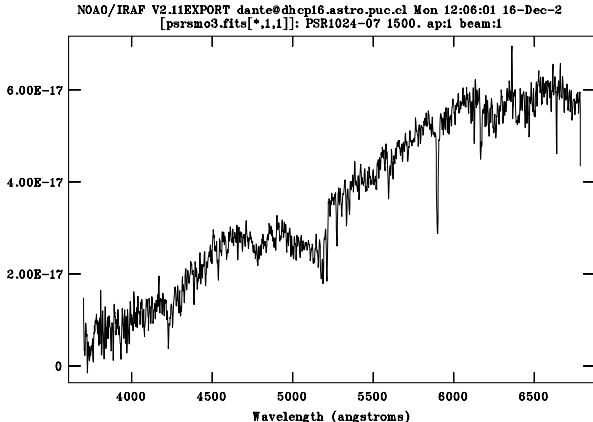
Since there are two point-like optical sources close to the nominal radio timing position of the pulsar, we examine their photometric colours and the spectrum of the brighter one to constrain their probable nature. The brighter star is in fact closer to the radio position of the pulsar, yet it is improbable that this is the optical counterpart.

The colours calculated for 1024-Br from the VLT observations, $V - R = 0.93$ and $V - I = 1.65$, do not match the optical and IR colors of white dwarfs very well. On the other hand, the visual colors V-R and V-I of 1024-Br can be approximately accounted for by a K5-type dwarf (with $M \sim 0.7M_{\odot}$, Allen 2000).

4.2.1. Spectroscopy of the brighter star 1024-Br

Because of the proximity of 1024-Br to the radio position of the pulsar (corrected for proper motion), spectroscopic observations of this object were carried out. The spectra were acquired with the Boller & Chivens spectrograph on the Magellan I Baade 6.5 m telescope at Las Campanas Observatory on the night of May 8, 2002. These observa-

Fig. 4. Spectrum of the brighter star 1024-Br near PSR J1024-0719. The spectrum corresponds to a typical early K-type dwarf star.



tions were taken during a spectroscopic survey of NGC 5128 globular clusters (see Minniti & Rejkuba 2002 for more details on the reduction procedures). We obtained two exposures of the source 1024-Br with 900 and 1500 seconds, respectively, at an airmass of 1.1. The measured seeing at the time of the observations was $0''.8$, and a slit width of $1''.0$ was used. The spectrophotometric standard LTT4816 observed at a similar airmass was used for the flux calibration, although the latter is uncertain due to the presence of thin cirrus during the night. The spectral reductions and measurements were carried out in IRAF, using the set of packages in CCDRED and TWODSPEC. The extracted spectra cover from 3700 to 6780\AA , with 1.5\AA pix^{-1} . The final average spectrum corrected for cosmic rays has a mean $S/N = 70 \text{ pix}^{-1}$, and is shown in Fig. 4. A few narrow absorption lines are present, and the spectrum corresponds to a typical early K-type dwarf star. Fig. 4 shows absorption features due to the Mg H band, the Mg5170 triplet, a weak Ca H and K doublet, the Na D doublet, as well as a number of iron lines such as Fe5270 and Fe5335. The lines of the hydrogen Balmer series are weak, and no prominent emission lines are present that would render this object peculiar in any way.

4.2.2. Binary companion or background star?

One can nevertheless ask if the star 1024-Br is physically associated with the pulsar in a possible binary system. This is ruled out, considering that a K5 dwarf star is likely to be as massive as $\approx 0.7M_{\odot}$ and the constraint from radio timing measurements of PSR J1024-0719.

A planet of mass m orbiting a pulsar of mass M_p in an orbit of semi-major axis a_p and period P_y years produces a periodic timing residual of semi-amplitude (see e.g. Phinney 1992)

$$\frac{a_p \sin i}{c} = 1700 \mu\text{s} \frac{m}{M_{\oplus}} \left[P_y \frac{1.4M_{\odot}}{M_p} \right]^{2/3} \sin i.$$

Monitoring of PSR J1024-0719 for over 3 years yields a timing residual smaller than $1 \mu\text{s}$ (Toscano et al. 1999a) which, for an orbital period smaller than this time span, constrains the mass of any companion to $m \sin i$ less than a thousandth of an Earth mass. A small but somewhat less constraining limit is obtained by allowing a longer orbital period ($P_{orb} = 2\pi/\Omega_{orb}$) and using the acceleration term in a binary orbit, $(P_0 \Omega_{orb}^2 a_p \sin i/c) \cos(\Omega_{orb} t)$, being bounded by the measured (apparent) period derivative of the pulsar spin \dot{P} . Here, P_0 is the intrinsic spin period. With the amplitude of the sinusoidally varying term and an orbital radius of 200 AU (corresponding to $1''$ in projection at $d = 200$ pc), we get a companion mass, $m \sin i < 4M_{\text{Jupiter}}$. Thus, 1024-Br, which is much brighter than even a Jupiter-like companion at this distance, is unlikely to be the binary companion of PSR J1024-0719. It is most likely a near-solar-mass background star located far beyond the 200 pc upper limit for the pulsar distance obtained from the Shklovskii effect.

4.3. The faint object 1024-Fnt

In the M_V vs. $V - I$ plane, we compare 1024-Fnt with the cooling track for a $0.6M_{\odot}$ white dwarf (DA or non-DA) given in Fig 6 of Bergeron et al. 1995. The $V - I$ colour is 0.73. The M_V is estimated by using $A_V = 0.11$ as above, and the distance modulus $\mu = 5 \log(d/\text{pc}) - 5 + A_V = 6.61$ for a distance of 200 pc, so that 1024-Fnt at that distance would have an absolute magnitude $M_V = 24.2 - 6.6 = 17.6$. This colour-magnitude position is well below the cooling curve of a $0.6M_{\odot}$ white dwarf (both a DA or a non-DA, i.e. hydrogen rich or non-hydrogen atmosphere WDs above a carbon core) as in Wood's (1995) evolutionary model. The multi-band spectrum of this object and its possible nature are discussed in the next section.

4.4. Implications for thermal and non-thermal models of the neutron star

If we take a single blackbody spectral distribution over a whole neutron star surface, the deepest (B-band) limit for PSR J1744-1134 (with $B \geq 26.9$ and $A_B = 0.07$) corresponds to a temperature

$$T_{\infty} \leq 2.1 \times 10^6 \text{ K} \left(\frac{d/0.36 \text{ kpc}}{R_{\infty}/10 \text{ km}} \right)^2,$$

where $T_{\infty} = T(1 - 2GM/Rc^2)^{1/2}$ and $R_{\infty} = R/(1 - 2GM/Rc^2)^{1/2}$ are the redshifted temperature and radius. We note that the X-ray detection (BT99) already constrains this temperature to much lower values.

We plot the multi-band flux densities of the faint source near the radio pulsar PSR J1024-0719, i.e. of 1024-Fnt as a function of the photon frequency in Fig. 3. For comparison, we also plot in this figure the corresponding multi-band flux densities from the Crab, LMC pulsar PSR B0540-69, and Vela (obtained from Percival et al. 1993; Middleditch et al. 1987 as restated by Nasuti et al. 1997;

and Nasuti et al. 1997 respectively). The remarkable similarity of the source 1024-Fnt with the multi-band flux densities of these well-known pulsars is noteworthy. For comparison in other wave-bands, the spectral (energy) index of Crab, γ ($I_\nu \propto \nu^{-\gamma}$) is consistent with $\gamma = 0$ at optical frequencies and varies from $\gamma = 1.1$ in the γ -ray region via 0.7 in the hard X-rays to 0.5 in the soft X-rays. The Crab spectral index changes sign and goes to $\gamma = -2$ in the far infrared and its radio frequency component is a separate component from the higher energy part (flux density decreasing with increasing frequency again) and has $\gamma = 2.7$ (Lyne & Smith 1990).

Similarly, the X-ray flux density of PSR J1024-0719 in the ROSAT band and its standard error were computed from the reported *un-absorbed* flux above (with the HRI count-rate) and an assumed photon index $\alpha = 2.3$ ($\gamma = 1.3$), close to that of the X-ray bright millisecond pulsar PSR J0437-4715 as seen by ROSAT. This gives a flux density of $4.1 \times 10^{-2} \mu\text{Jy}$ with the centroid at 0.33 keV ($7.97 \times 10^{16} \text{ Hz}$) and an effective bandwidth of 0.23 keV. The radio flux densities at three frequencies (400 MHz, 600 MHz and 1400 MHz) for both pulsars were obtained from Bailes et al. (1997). To guide the eye in Fig. 5 for the multi-band data, we also draw a few representative spectra: a) a power law with photon index $\alpha_r = 2.85$ ($\gamma = 1.85$), which matches the radio data well; b) a power-law spectrum of index $\alpha_{ox} = 1.55$ connecting the highest frequency optical datum to the X-ray, and c) a blackbody spectrum of temperature $T_\infty = 2.1 \times 10^6 \text{ K}$ from a heated cap ($R_\infty^{\text{core}} = 0.06 \text{ km}$) of the neutron star surface at a distance of $d = 0.2 \text{ kpc}$. It is clear that a single power-law connecting the optical emission from 1024-Fnt and the X-ray emission from PSR J1024-0719 shall involve a minimum photon index of 1.55 and the maximum limit on the hot polar cap temperature $T \leq 2.1 \times 10^6 \text{ K}$ for a hot-spot of radius 60 m. On the other hand, the optical magnitude in the U-band implies for a single blackbody function for the entire neutron star surface a temperature $T_\infty \leq 4 \times 10^4 \text{ K} / \ln\{1 + 4.35 \times 10^{-4} [(R_\infty/10 \text{ km})/d_{\text{kpc}}]^2\}$

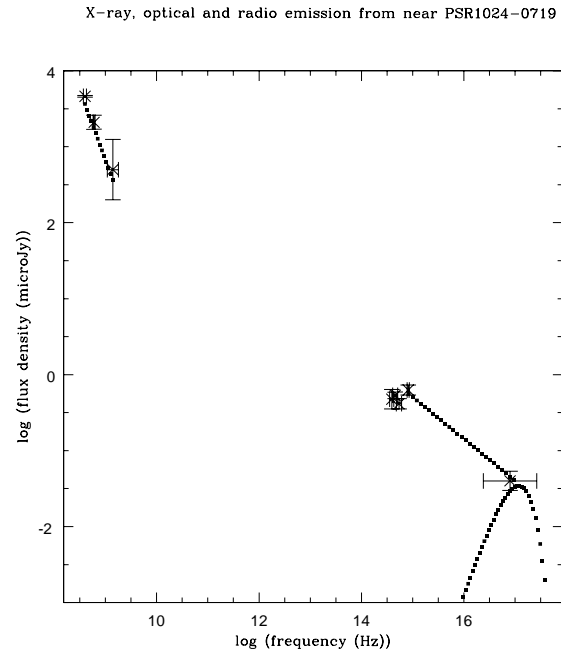
$$\approx 3.7 \times 10^6 \text{ K} \left(\frac{d/0.2 \text{ kpc}}{R_\infty/10 \text{ km}} \right)^2,$$

where the latter expression corresponds to the Rayleigh-Jeans limit. This limit is again much less constraining than that obtained from the X-ray data of BT99.

5. Discussion

Non-thermal models for optical radiation for slower pulsars like the Crab ascribe it to synchrotron emission (see Pacini 1971 and Pacini & Salvati 1987) by relativistic particles near the light cylinder radius at very small pitch angles ($\Psi \ll 1/\gamma$, where the Lorentz factor may be $\gamma \sim 10^2 - 10^3$; Crusius-Wätzel et al. 2001). Malov & Machabeli (2001) show that finite pitch angles of the plasma particles appear in the outer magnetosphere near the light cylinder due to an instability associated with the cyclotron resonance condition being fulfilled

Fig. 5. Multiwaveband emission from near PSR J1024-0719. Included are the radio flux densities at 400, 600 and 1400 MHz; the optical data (this paper) of 1024-Fnt; and the ROSAT HRI X-ray data. Two illustrative power laws and a blackbody curve are shown. The blackbody emission is from a heated region of the neutron star polar cap of radius 60 m and temperature $2 \times 10^6 \text{ K}$, at a distance of 50 pc.



there. They further show that pulsars with shorter periods such as the millisecond pulsars attain harder spectra and higher peak frequencies. Although millisecond pulsars have much smaller surface magnetic fields than slower pulsars, they also have smaller corotating magnetosphere radii, making the dipolar fields at light cylinder distances (a key parameter for particle acceleration models) similar to those of slower pulsars. Thus, in many of the millisecond pulsars, acceleration of particles in outer gaps sustained by pair creation by GeV gamma-rays may still be operative as in high spin-down luminosity pulsars (Cheng, Ho, & Ruderman 1986). The non-thermal power-law component due to pair-gap discharge is expected to scale with the Goldreich-Julian particle flux $\dot{N}_{GJ} = (\mathbf{\Omega} \cdot \mathbf{B})/2\pi e$ from the magnetosphere (see Harding 1981 or Thompson 1998). For some millisecond pulsars \dot{N}_{GJ} is in excess of that of PSR B0656+14, which is found to be a gamma-ray, X-ray and optical pulsar. We note that for our target pulsars, the Goldreich-Julian particle fluxes are close to that of Geminga (within a factor of two) from which optical pulsations have possibly been seen (Shearer et al. 1998).

Scaled to the period ($P = 5.16 \text{ ms}$) and the surface magnetic field ($B_0 \sim 10^{8.1}$) in PSR J1024-0719, expres-

sions (33) and (35) of Crusius-Wätzels et al. (2001) imply that

$$\frac{I_{\nu}^{opt}}{I_{\nu}^X} = 6 \times 10^{-2} \frac{(\Psi_{opt}/10^{-3})^2 (\nu_{opt}/10^{15} \text{Hz}) (P/5.16 \text{ms})^{3/2}}{(\Psi_X/0.1)^{3/2} (\nu_X/10^{17} \text{Hz})^{1/2} (B_0/10^{8.1} \text{G})^{1/2}}$$

This ratio is smaller than what is found for the optical to X-ray flux density ratio of PSR J1024-0719 (see Fig. 5), i.e., $I^{opt}/I^X \sim 15$ instead of 6×10^{-2} , if the object 1024-Fnt is indeed the pulsar optical counterpart, and the observed emission is primarily pulsed. This indicates that in millisecond pulsars the average pitch angles responsible for optical radiation are larger, $\Psi_{opt} \sim 10^{-2}$.

In middle-aged ($\tau \approx 10^5 - 10^6$ yr) and even older neutron stars, at least a part of the high-energy radiation is due to thermal emission from the neutron star's surface. The faint measured UV flux from the slow pulsar PSR B0950+08 indicates that a surface temperature $T_s \sim 3 - 5 \times 10^4$ K could be appropriate for an old pulsar, assuming a blackbody fit and thermal radiation arising from the entire NS surface (Pavlov, Stringfellow, & Cordova 1996). Even more than for this relatively old pulsar, the much older age of the millisecond pulsars implies that these stars have almost certainly radiated away any "fossil" heat due to the original collapse or to subsequent accretion from a binary companion. However, their high spin-down power implies that internal dissipation is probably active, keeping their surface at a higher temperature (e.g., Cheng et al. 1992, Reisenegger 1995, Reisenegger 1997, Larson & Link 1999, Schaab et al. 1999). Unfortunately, the optical band limits obtained here are not strongly constraining for a blackbody of size similar to or smaller than a NS.

The object 1024-Fnt has a multi-band spectrum which is unusual and characteristic of pulsars, such as the Crab, Vela and PSR B0540-69. Given its proximity to the radio position of PSR J1024-0719 and the considerable astrometric uncertainty, only timing analysis with high time resolution can unambiguously define its nature.

6. Conclusions

Among the isolated millisecond pulsars, none so far have been shown to pulse in the optical. Deep exposures carried out with the VLT of the field of the nearby, isolated pulsar PSR J1744-1134 in multiple bands do not show a plausible optical counterpart. We derive upper limits to the surface temperature of the underlying neutron star at the likely distance of the pulsar. In the field of view of PSR J1024-0719, we detect two objects close to the radio position of the pulsar. We argue, based on photometry and spectroscopy, that the brighter object is a background early K-type dwarf star. The fainter object, 1024-Fnt, has a multi-band spectrum which is unusual and characteristic of pulsars. Future high time resolution observations may unambiguously define its nature by the detection of optical pulses.

Acknowledgements. We thank M. Cristina Depassier for her role in the formation of this collaboration and Marina Rejkuba for sharing with us the Magellan I spectroscopic data obtained in collaboration with D. Minniti. A. Ray thanks Malvin Ruderman for discussions on optical radiation from pulsars at the Aspen Center for Physics and Poonam Chandra for her comments on the manuscript. A. Reisenegger thanks Marten van Kerkwijk for advice about astrometry with the VLT, Frédéric Courbin for help with the "p2pp" and René Méndez for useful discussions. A. Reisenegger's and G. Hertling's work was supported by FONDECYT grant No. 1020840, and H. Quintana's and D. Minniti's by the FONDAP Center for Astrophysics. At Tata Institute, this work was a part of the Five Year Plan Projects 10P-201 and 9P-208[a].

References

Allen C. W. 2000, "Allen's Astrophysical Quantities", (4th. edition), Ed. A. N. Cox, Springer.

Alpar M. A., Cheng A., Ruderman M.A., Shaham J. 1982, Nature, 300, 728.

Bailes M., Johnston S., et al., ApJ 481, 386.

Becker W., Aschenbach B. 2002, in "Neutron stars, pulsars and supernova remnants", WE-Heraeus Seminar, p.64.

Becker W., Trümper J. 1997 A&A 326, 682.

Becker W., Trümper J. 1999, A&A 341, 803-817: BT99.

Bergeron P., Wesemael F., Beauchamp A. 1995, PASP 107, 1047.

de Boer K. S., et al. 1987, in "Exploring the Universe with IUE", ed. Y. Kondo, D. Reidel and Company.

Cheng K. S., Chau W. Y., Zhang J. L., Chau H. F. 1992, ApJ 396, 135.

Cheng K. S., Ho C., Ruderman M. A. 1986, ApJ 300, 500.

Crusius-Wätzels A. R., Kunzl T., Lesch H. 2001, ApJ 546, 401.

Fomalont E. B., Goss W. M., Manchester R. N., Lyne A. G., Justtanont K. 1992, MNRAS, 258, 497.

Fomalont E. B., Goss W. M., Manchester R. N., Lyne A. G. 1997, MNRAS, 286, 81.

FORS1+2 User Manual, Paranal Observatory Very Large Telescope, European Southern Observatory Manual, p. 87.

Harding A. 1981, ApJ 245, 267.

Hewish A., Bell S. J., Pilkington J.D.H., Scott P.F., Collins R.A. 1968, Nature, 217, 709.

Landolt A.U. 1992, AJ, 104, 340.

Larson M. B., Link B. 1999, ApJ 521, 271.

Lyne A. G., Graham-Smith F. 1990, "Pulsar astronomy", Cambridge Univ. Press.

Ma C. et al. 1998, AJ 116, 516.

Malov I., Machabeli G.Z. 2001, ApJ 554, 587.

Massey P., Davis L. E. 1992, "A Users guide to stellar photometry IRAF".

Mathis J. 1999, "Allen's Astrophysical Quantities", A. N. Cox (Editor), Springer-Verlag.

Minniti D., Rejkuba M. 2002, ApJ 575, L59.

Middleditch J., Pennypacker C.R. Burns M.S. 1987, ApJ 315, 142.

Monet D., Bird A., et al., Vizier On-line Data Catalog: I/252. U.S. Naval Observatory Flagstaff Station (USNOFS).

Nasuti F.P., Mignani R., Caraveo P.A., Bignami G.F. 1997, A&A 323, 839.

Pacini F. 1971, ApJ 163, L17.

Pacini F., Salvati M. 1987, ApJ 321, 447.

Pavlov G. G., Stringfellow G. S., Cordova F. A. 1996, *ApJ* 467, 370.

Percival J.W., et al. 1993, *ApJ* 407, 276.

Phinney E. S. 1992, *Phil. Trans. Roy. Soc. Lond. A* 341, 39.

Reisenegger A. 1995, *ApJ* 442, 749.

Reisenegger A. 1997, *ApJ* 485, 313.

Rots A. H., Jahoda K., Macomb D., et al. 1998 *ApJ* 501, 749.

Ruderman M. A., Sutherland P. G. 1975, *ApJ* 196, 51.

Ruiz M. T., Bergeron P. 2001, *ApJ* 558, 761.

Schaab Ch., Sedrakian A., Weber F., Weigel M. K. 1999, *A&A*, 346, 465.

Shklovskii I. S. 1970, *Soviet Astron.*, 13, 562.

Shearer A., Golden A. 2002, in “Neutron stars, Pulsars and Supernova Remnants”, WE-Heraeus Seminar, Eds. W. Becker et al., MPE Report 278, p. 44.

Shearer A., Golden A. 2001, *ApJ* 547, 967.

Shearer A., Golden A., et al. 1998, *A&A* 335, L21.

Staelin D. H., Reifenstein E. C. 1968, *Science*, 162, 1481.

Taylor J. H., Cordes J. M. 1993, *ApJ* 411, 674.

Thompson D. J. 1998, in “Neutron stars and pulsars”, ed. N. Shibasaki et al., Universal Academic Press (Tokyo).

Toscano M., Britton M. C., Manchester R. N., et al. 1999a, *MNRAS*, 307, 925.

Toscano M., Britton M. C., Manchester R. N., et al., 1999b, *ApJ* 523, L171.